

Appendix from S. Dasgupta and S. Mukherjee, “Brittle Shear Tectonics in a Narrow Continental Rift: Asymmetric Nonvolcanic Barmer Basin (Rajasthan, India)” (J. Geol., vol. 125, no. 5, p. 000)

Structural and Tectonic Information Presented by Oil Industry Geoscientists at Undisclosed Coordinates from Barmer Basin

1. The Aishwarya/Aishwariya oil field consists of a rotational fault block with a 10° dip toward the east. A major bounding fault system exists to the west and NW of it (Chaliha et al. 2016).

2. From the Raageshwari oil field, three sets of extensional fractures, trending NE, NW, and WSW, have been identified. The ENE has been correlated with Barmer basin extension. Geomechanical modeling shows that present-day strike-slip tectonics prevails in the Barmer basin. The horizontal stress anisotropy in the northern part of the Barmer basin is greater than that in the central part (Dash et al. 2016).

3. Synsedimentary faulting, gravity collapse, and low-angle listric faults are reported from the Barmer Hill Formation (Pal et al. 2016).

4. The Bhagyam field is a tilted fault block dipping at 10°–15° toward the SE and is bound by NNE- and WSW-trending faults. Faults show reducing throw at a shallower level, along with an increase in secondary splay faults, both synthetic and antithetic. A dip illumination map revealed more intrareservoir faults (Tiwari et al. 2014).

q53

Supplementary Figures and Table

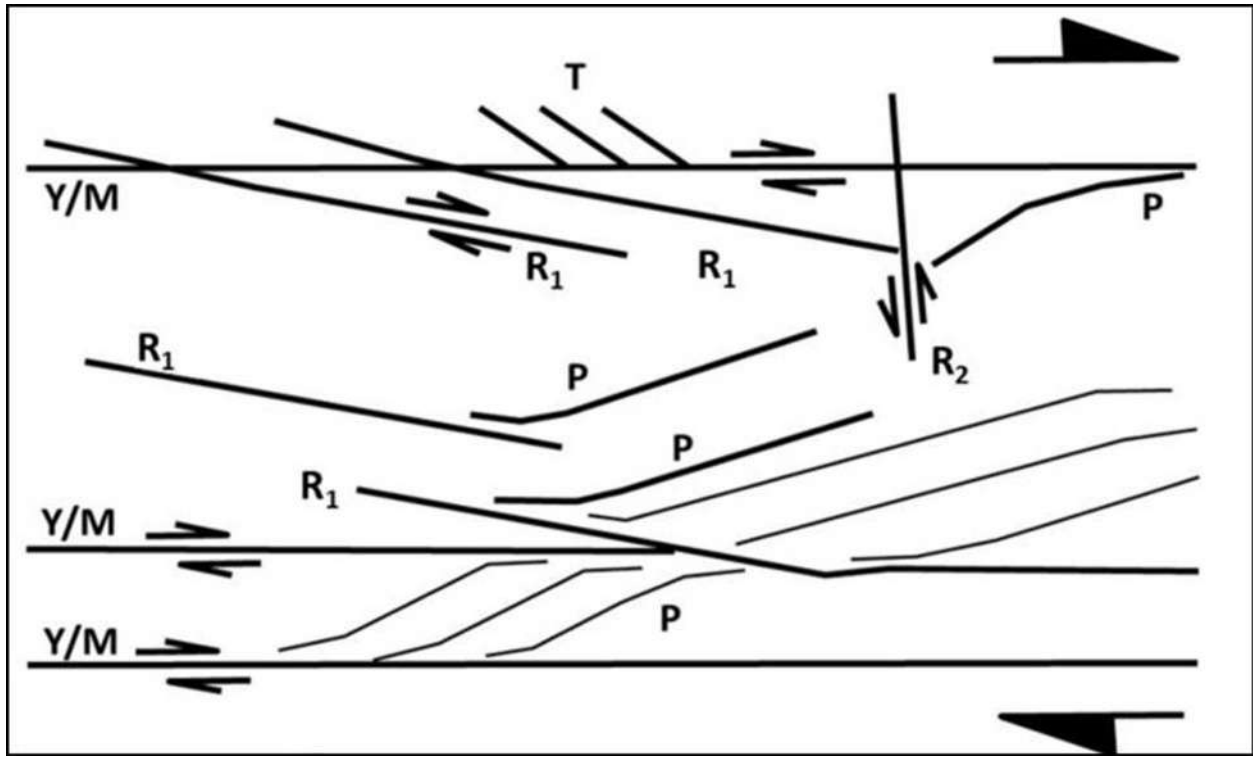


Figure A1. Typical brittle shear zone associated with different types of fractures, that is, Y- and P-planes and Riedel shear system R_1 , R_2 , P, T, and M fractures. M = average slip surface; P = primary shear fractures; R = Riedel shears; T = extension fractures (Passchier and Trouw 2005; also see Misra and Mukherjee 2015).

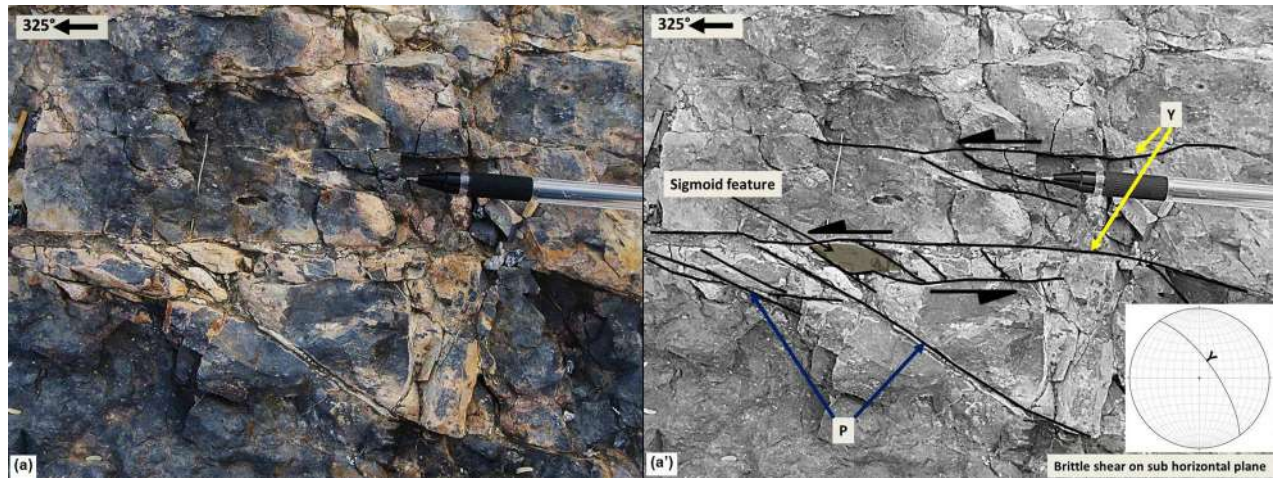


Figure A2. Uninterpreted (*a*) and interpreted (*a'*) images of sinistral brittle shear with distinct Y- and P-planes, within Malani rhyolite, on a subhorizontal surface. The Y-plane trends NW (attitude: 145° strike, 71° dip, 55° dip direction). Part of a pen (~12 cm) is shown for scale. *Inset*, stereonet plot of the Y-plane. Location: SW of Ratanada Temple in the Barmer hill area, Barmer town; near L1 in figure 1A.

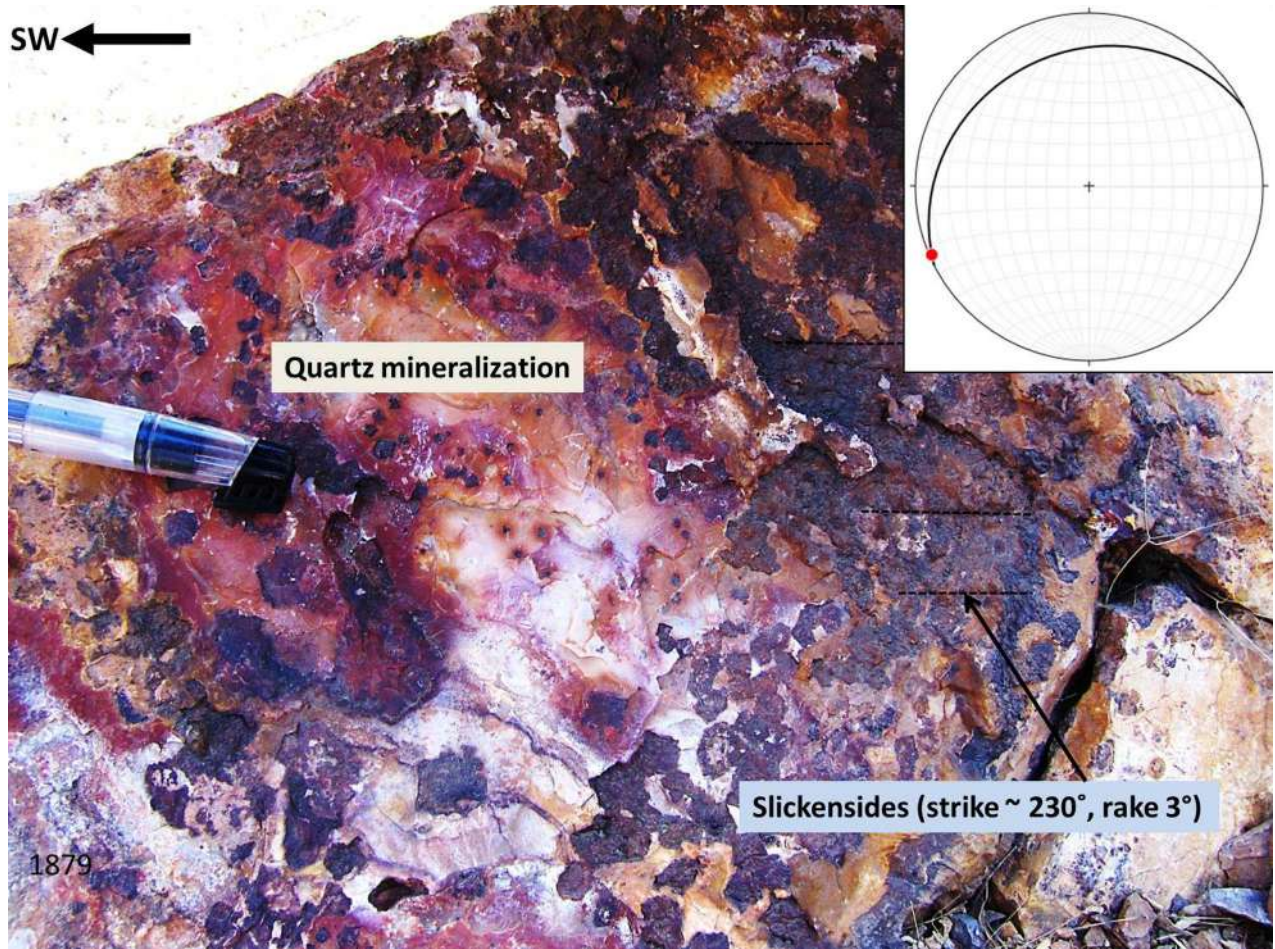


Figure A3. SW-trending fault-plane surface (attitude: 243° strike, 23° dip, 330° dip direction) with secondary quartz mineralization on one side and slickenside striations on the other. Striations (rake: 3°; trend: ~230°) indicate strike-slip movement, although the slip direction could not be deciphered. *Inset*, stereonet plot of the fault plane with slickenside lineation. Part of a pen (~4 cm) is shown for scale. Location: west of Ratanada Temple in the Barmer hill area, Barmer town; near L1 in figure 1A.

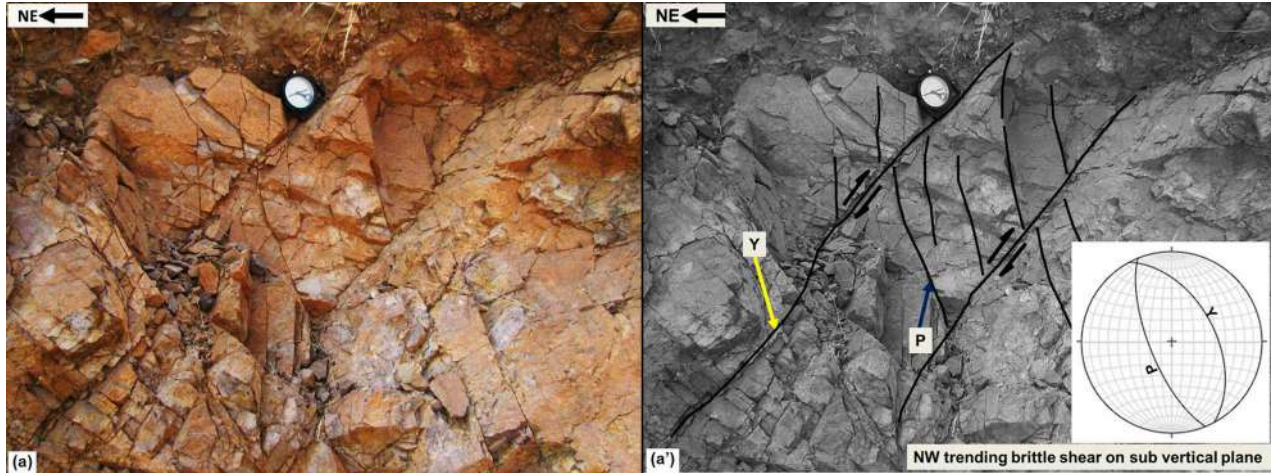


Figure A4. Uninterpreted (a) and interpreted (a') NW-trending brittle shear with well-developed P-plane (attitude: 158° strike, 70° dip, 248° dip direction) and Y-plane (attitude: 332° strike, 50° dip, 62° dip direction); top-to-SW (up) slip is observed on a subvertical surface. A clinometer ~8 cm in diameter is shown for scale. *Inset*, stereonet plot of the Y- and P-planes. Location: cutout section in roadside exposure toward Genhoo village; near L2 in figure 1A.

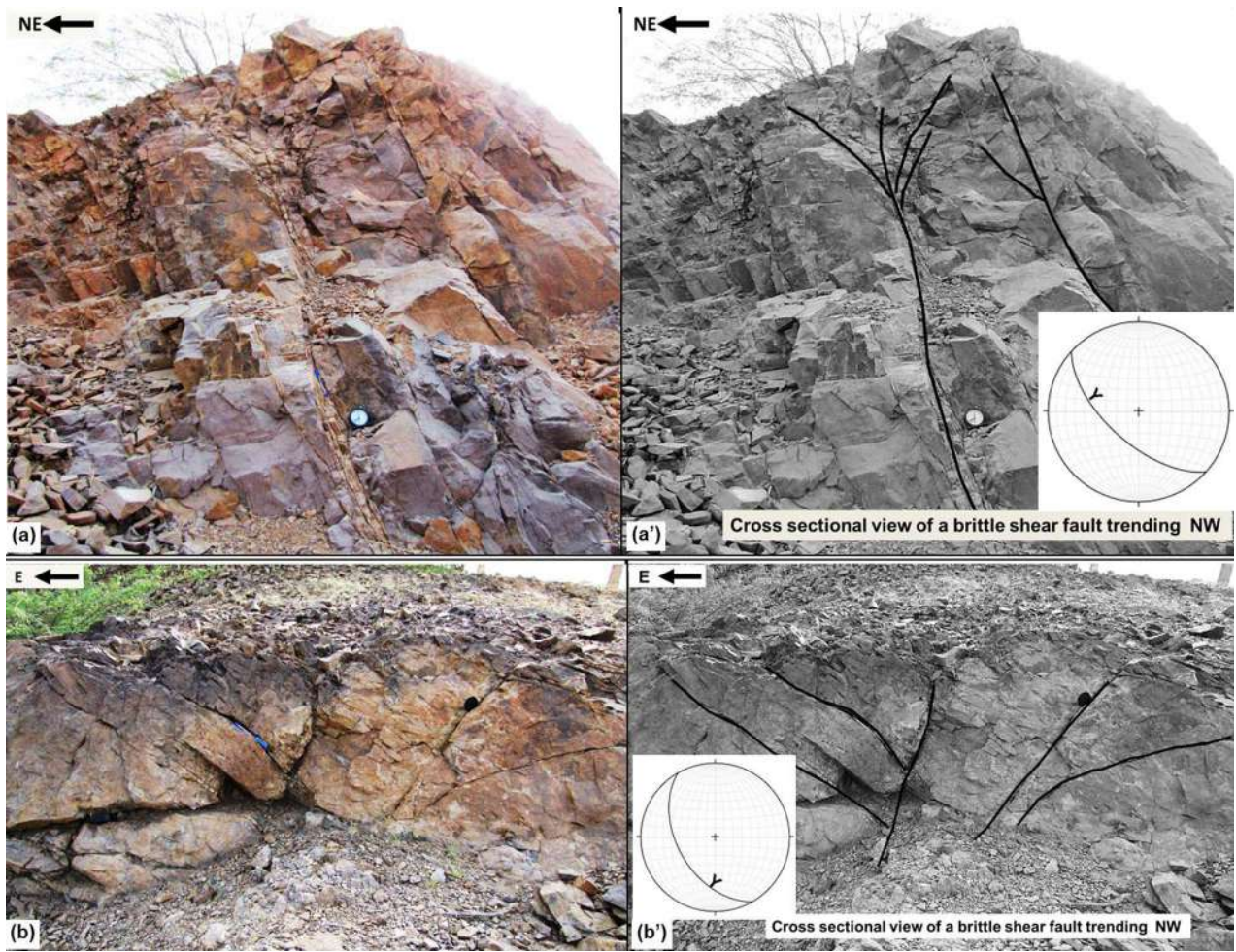


Figure A5. Uninterpreted (*a, b*) and interpreted (*a', b'*) roughly vertical cross sections of NW-trending strike-slip brittle shear. The P- and the Y-planes (*top*: attitude: 132° strike, 62° dip, 222° dip direction; *bottom*: attitude: 150° strike, 48° dip, 240° dip direction) together constitute a positive flower structure. A clinometer ~ 8 cm in diameter and a pen ~ 15 cm long are shown for scale in the top and bottom photos, respectively. *Insets*, stereonet plots of the Y-planes. Location: roadside near Gehnoo village; near L2 in figure 1A.

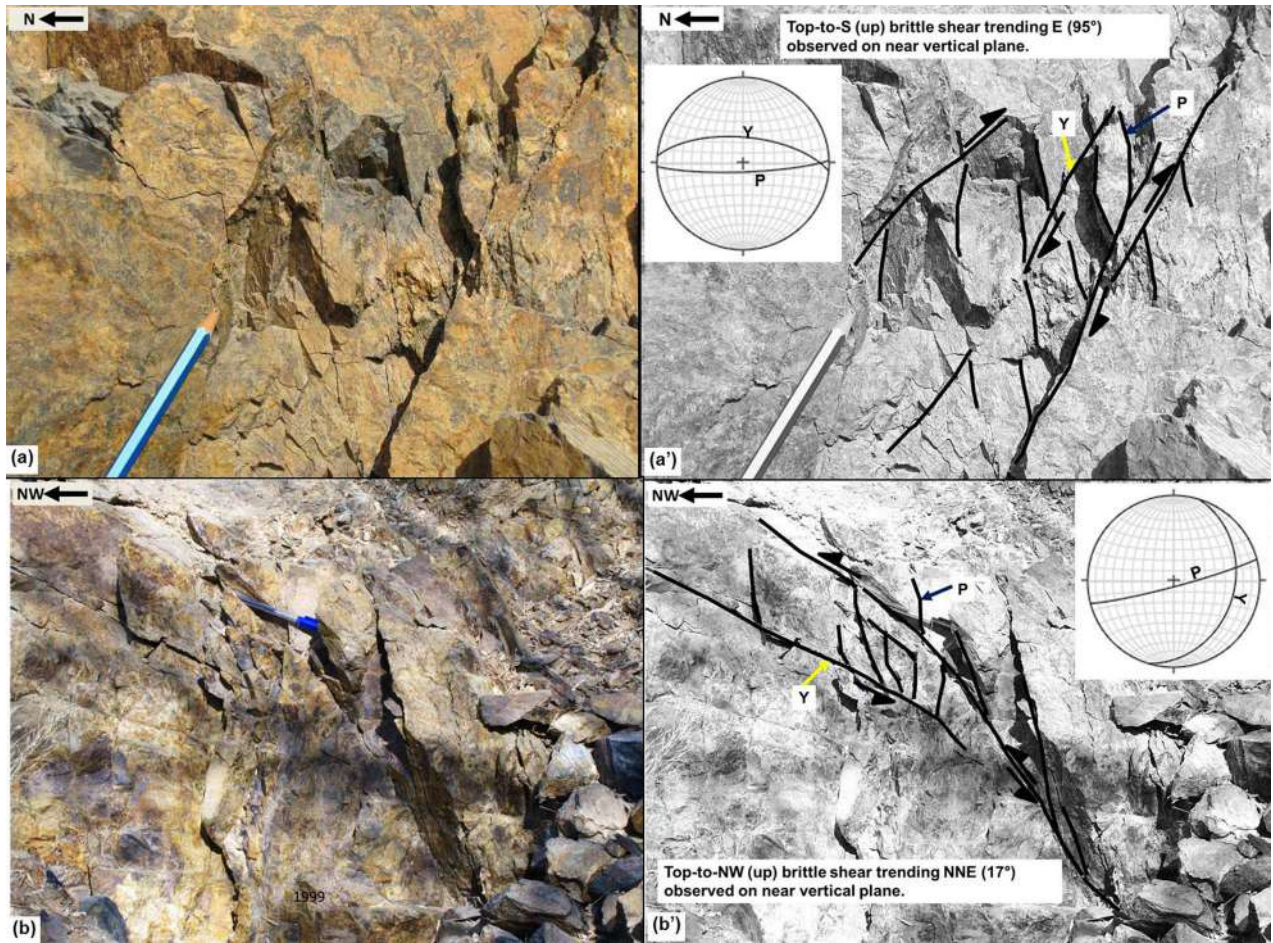


Figure A6. *Top*, uninterpreted (a) and interpreted (a') photos of ESE-trending top-to-right brittle shear with a P-plane (attitude: 268° strike, 82° dip, 178° dip direction) and a Y-plane (attitude: 95° strike, 65° dip, 5° dip direction), observed on a subvertical surface. *Bottom*, uninterpreted (b) and interpreted (b') photographs of NNE-trending top-to-south (up) brittle shear with a P-plane (attitude: 75° strike, 85° dip, 165° dip direction) and a Y-plane (attitude: 197° strike, 30° dip, 107° dip direction), observed on a subvertical surface. Part of a pencil (~ 14 cm) and a pen ~ 15 cm long are shown for scale in the top and bottom photographs, respectively. *Insets*, stereonet plots of the Y- and P-planes. Though not crosscutting, they probably develop a conjugate set of reverse faults. Location: outcrop section in Jasai village area, north of the Jasai railway station; near L3 in figure 1A.

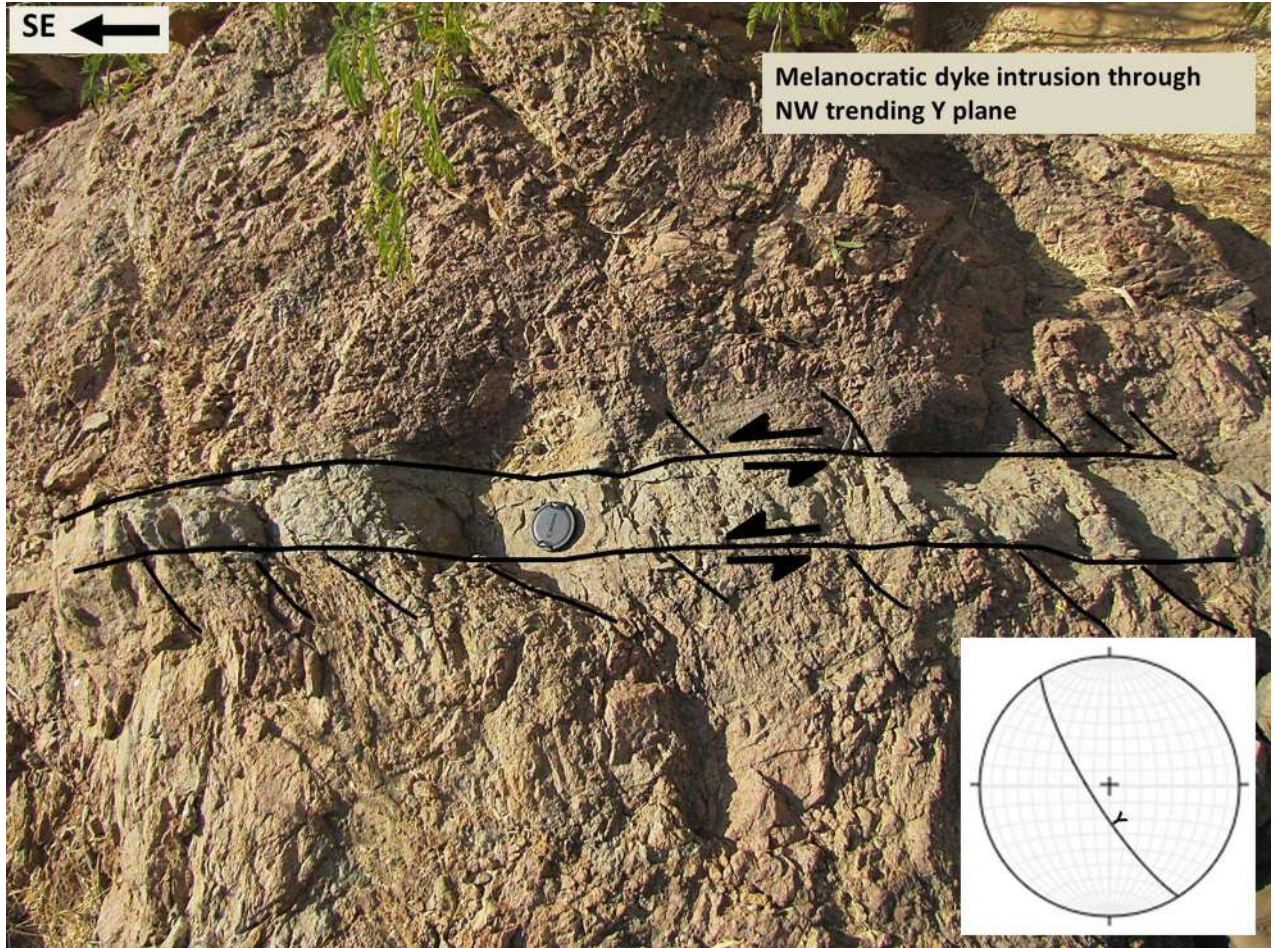


Figure A7. NW-trending melanocratic dike intruding the granite along the NW-trending Y-plane (attitude: 328° strike, 78° dip, 238° dip direction), observed on a subhorizontal surface. Sinistral shear is indicated. A camera lens cover ~ 6 cm in diameter is shown for scale. *Inset*, stereonet of Y-plane. Location: granitic outcrop of the Malani Igneous Suite NW of Dhorimana village; near L4 in figure 1A.

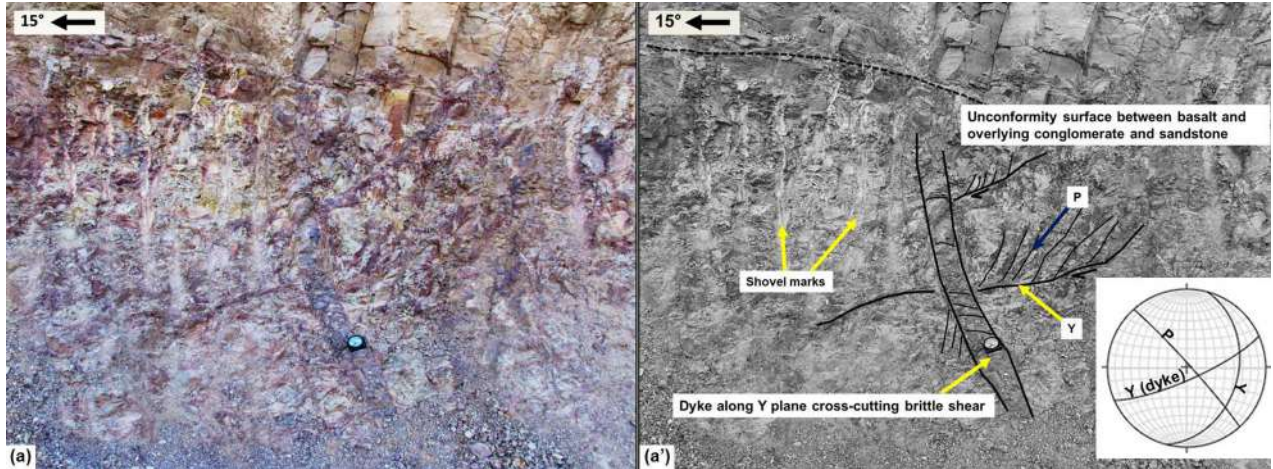


Figure A8. Uninterpreted (*a*) and interpreted (*a'*) photos of brittle deformation observed on a subvertical section of the older Early Cretaceous basalt below the Ghaggar-Hakra Formation. A dike intruded through the Y-plane (attitude: 246° strike, 78° dip, 156° dip direction) cuts across older brittle shears trending south/SSW associated with a Y-plane (attitude: 195° strike, 35° dip, 105° dip direction) and a P-plane (attitude: 138° strike, 86° dip, 48° dip direction), with a top-to-SSW slip. This dike terminates abruptly at the unconformity surface of the basalt overlain by basal conglomerates of the Ghaggar-Hakra Formation. A clinometer ~8 cm in diameter is shown for scale. Brittle shears were carefully discriminated from shovel marks. *Inset* stereonet of Y- and P-planes. Location: NW part of the lower Sarnu/Sarnoo hill area; near L5 in figure 1A.

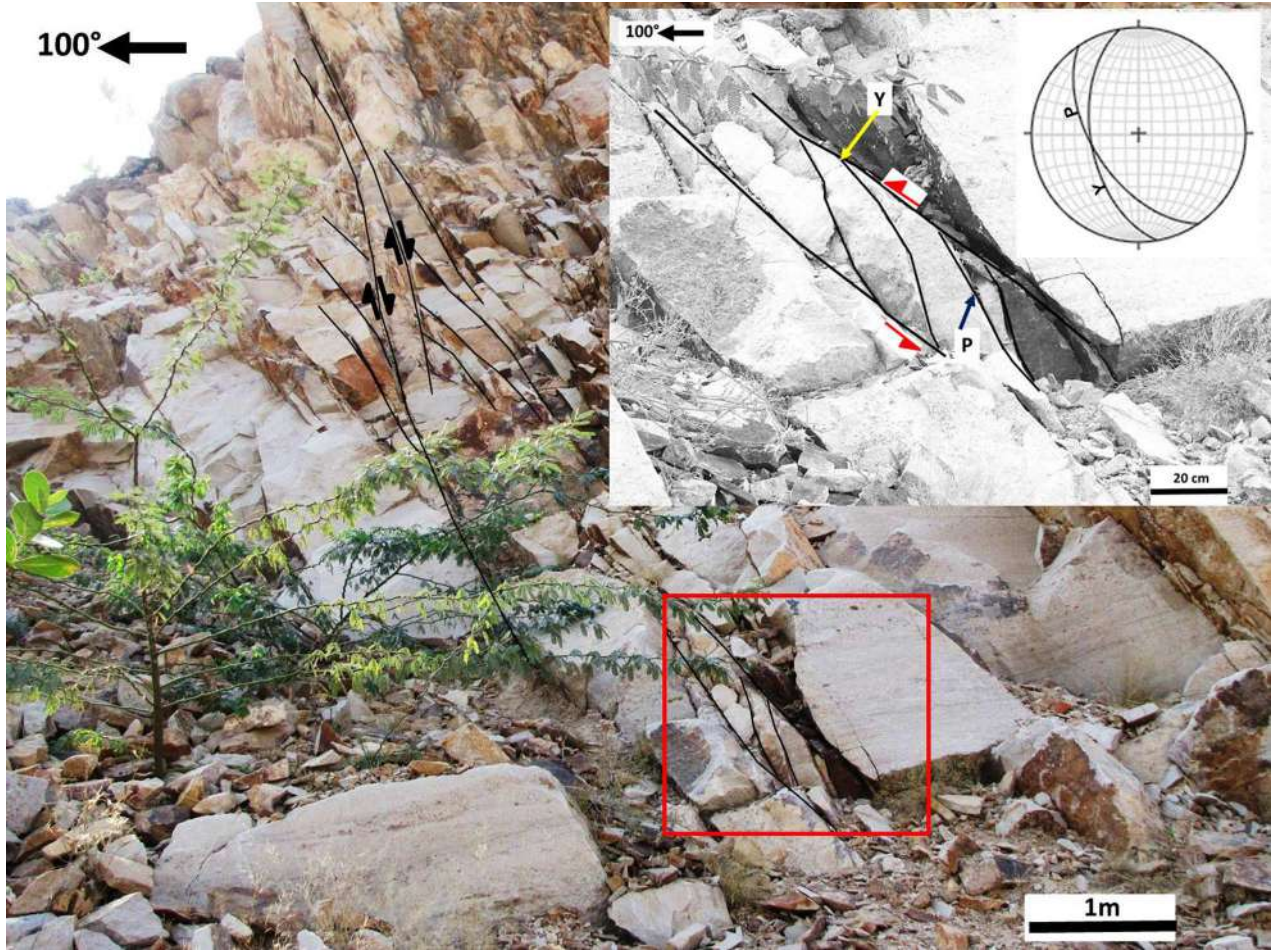


Figure A9. Nearly vertical section of the lower part of the Ghaggar-Hakra Formation, depicting SE-trending brittle shear in a sandstone body with Y- and P-planes. The larger fault, at left (>3 m), shows a top-to-roughly-NNW brittle shear (normal faulting; Y-plane attitude: 165° strike, 67° dip, 255° dip direction). The smaller fault, marked by red box (close-up in inset), in the lower part of the hanging wall is a top-to-roughly-ESE reverse fault. The attitudes of reverse faulting with Y- and P-planes are 170° strike, 53° dip, 260° dip direction and 146° strike, 55° dip, 236° dip direction, respectively. *Subinset*, stereonet of Y- and P-planes. Location: western part of the Sarnu/Sarnia hill area; near L5 in figure 1A.

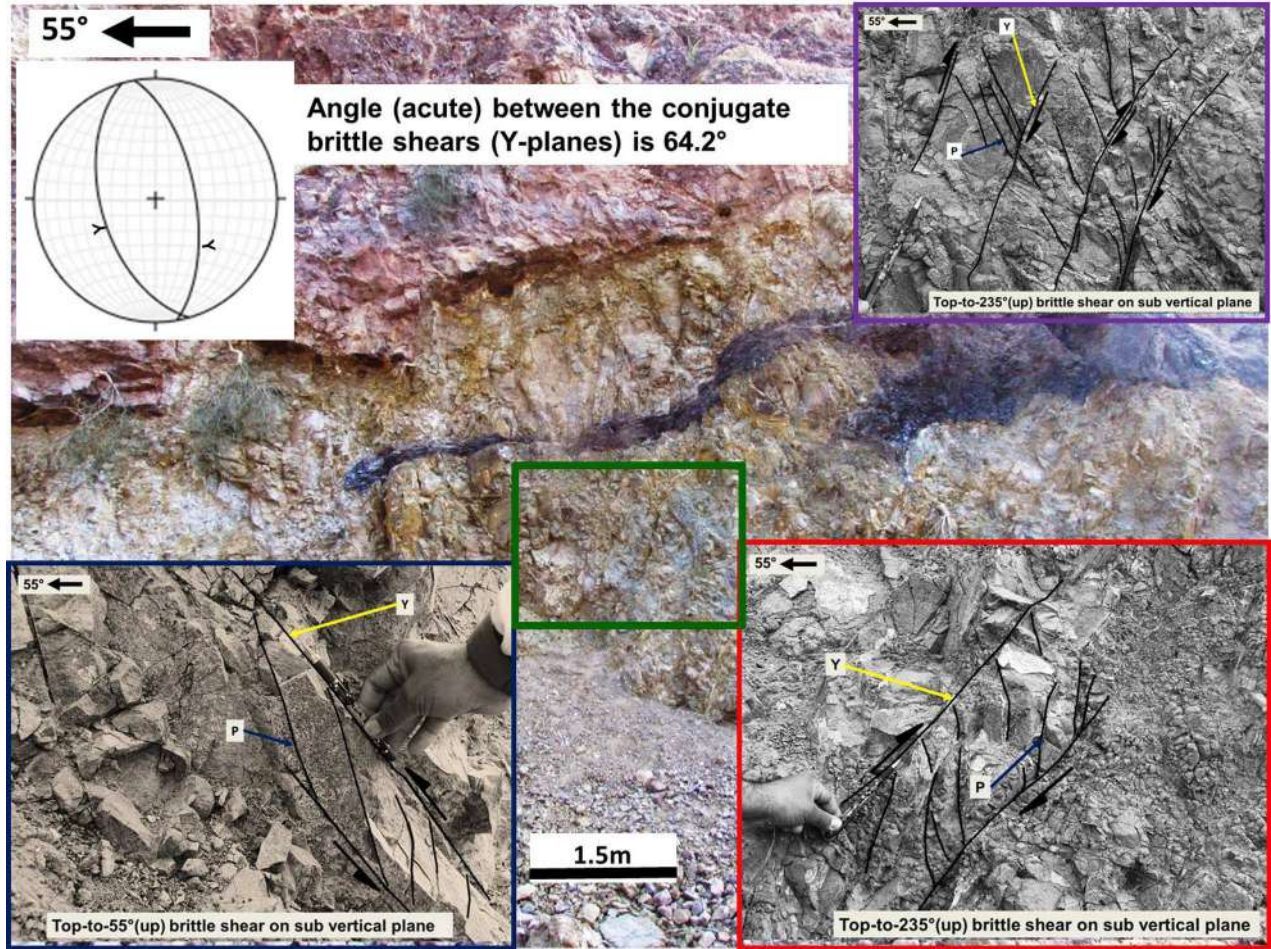


Figure A10. Set of brittle shears associated with P- and Y-planes observed in the lower part of the Ghaggar-Hakra Formation below the basalt sill body, within green box. Close-ups of conjugate reverse faults are shown in the other boxes. Blue box: top-to-roughly-NE slip; Y-plane attitude: 164° strike, 53° dip, 254° dip direction; P-plane attitude: 175° strike, 78° dip, 85° dip direction. Red box: top-to-roughly-SW slip; Y-plane attitude: 170° strike, 63° dip, 80° dip direction; P-plane attitude: 220° strike, 64° dip, 130° dip direction. The shear sense in the purple box is another example of the latter. The conjugate reverse faults do not crosscut. A pen ~16 cm long is shown for scale in the close-ups. The acute angle between the conjugate reverse faults is 64.2°, as per the stereonet plot (*inset*). Location: west-facing outcrop hillock 600 m NE of Sarnu/Sarnoo village; near L5 in figure 1A.

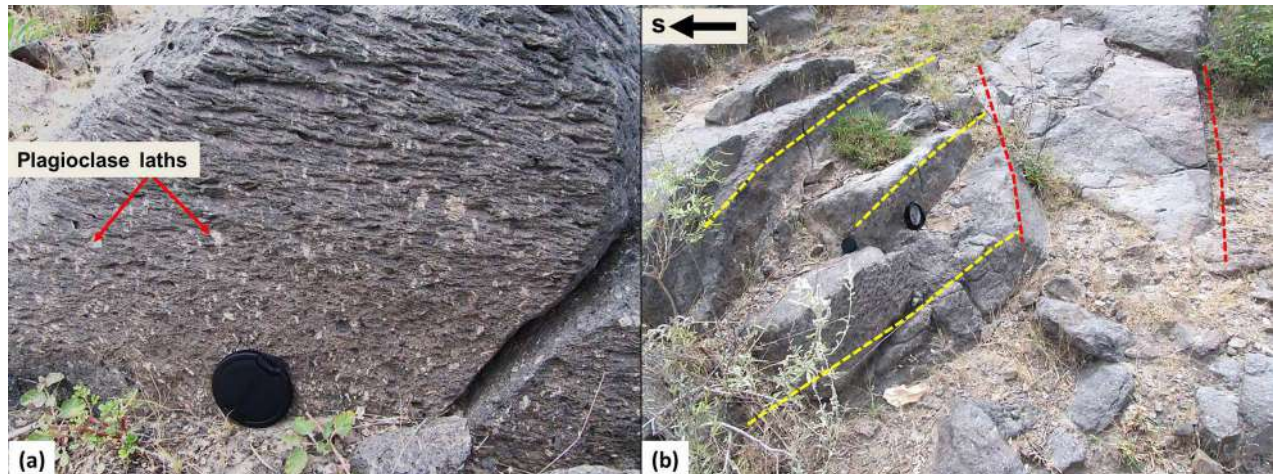


Figure A11. *a*, Large plagioclase laths on a fracture surface of the basalt body possibly indicate a linear igneous flow. A camera lens cover ~ 6 cm in diameter is shown for scale. *b*, Two prominent sets of tectonic fractures, trending NE and NW, identified in the basalt outcrop. The NW-trending fractures are more prevalent. A clinometer ~ 8 cm in diameter is shown for scale. Location: near a primary school, ~ 1 km SE of Sarnu/Sarnoo village; near L5 in figure 1A.

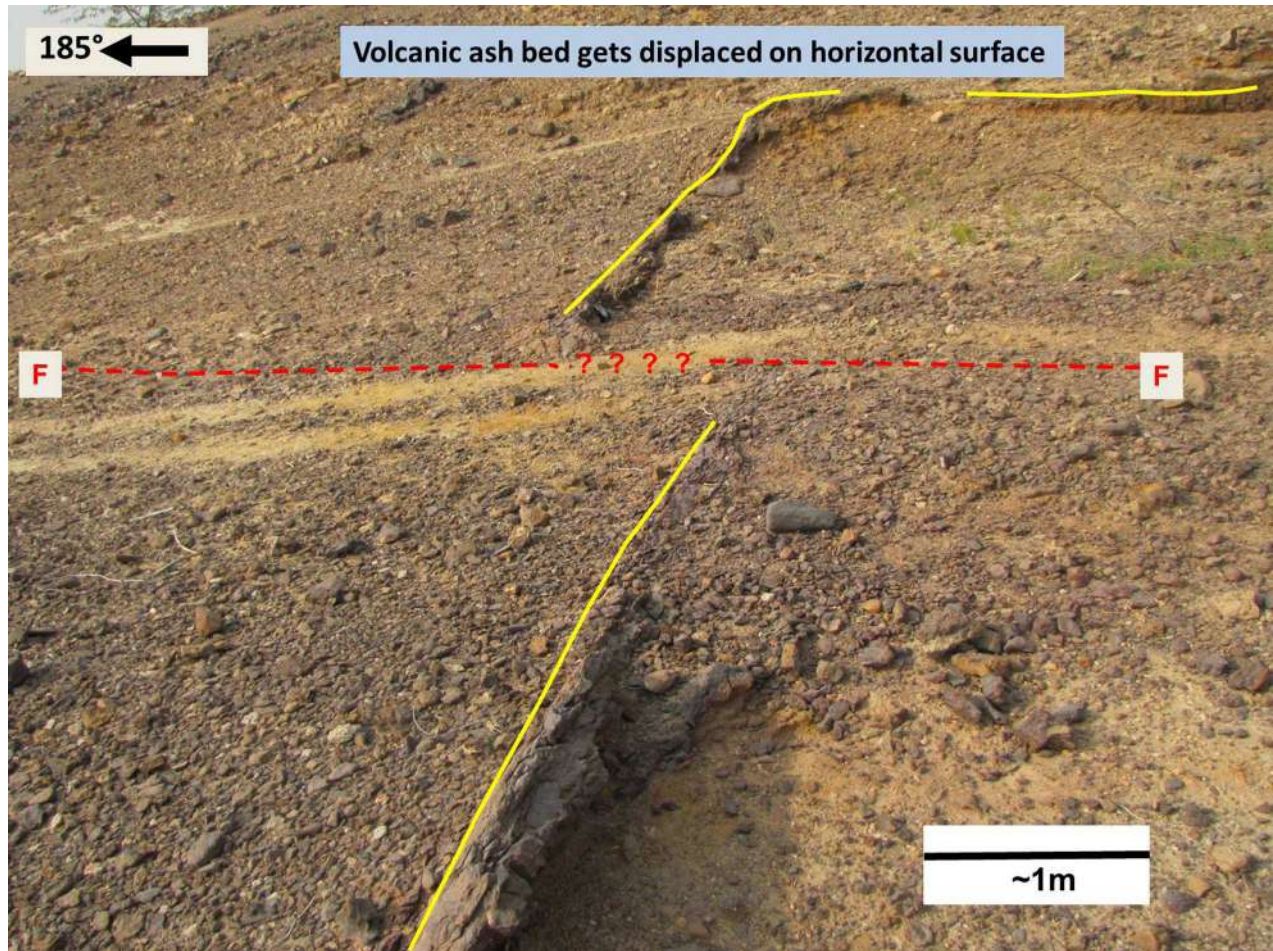


Figure A12. Left-laterally displaced volcanic ash bed by probable sinistral strike-slip fault (dashed red line), as observed on subhorizontal section. Location: 110 km north of Barmer town, 2–3 km west of National Highway 15; near L7 in figure 1A.

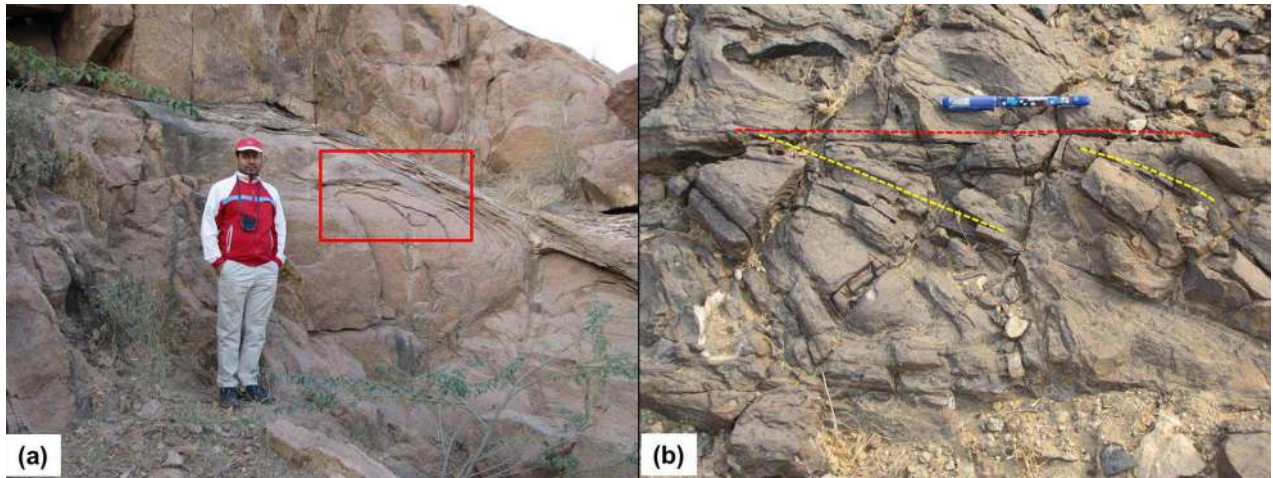


Figure A13. *a*, Weathering-related fracture planes resembling P-planes in granite, not considered brittle shear. S. Mukherjee (174 cm) is shown for scale. *b*, Tectonic fracture associated with weathering/cooling-related fractures resembling P-planes, not considered for brittle shear interpretation. A pen ~16 cm long is shown for scale.

Table A1. Stratigraphy of the Barmer Basin

Age, series, formation	Lithology/key features
Neogene–Quaternary:	
Pliocene–Pleistocene:	
Uttarlai	Part of thermal sag, comprised of alluvium and aeolian deposits
Neogene:	
Miocene:	
Jagadia	Part of thermal sag, comprised of alluvium and aeolian deposits
Paleogene–Neogene:	
Oligocene–Early Miocene	Major hiatus
Paleogene:	
Eocene:	
Nagarka	Poorly understood because of very few exposures, mostly undrilled; consists of dark shales similar to those of Akli Fm.
Kapurdi	Lacustrine fuller’s earth deposits with alternate layers of shallow marine limestone
Matajika Dungar	Shallow marine hard sandstone; mixed bentonitic clay bands at the base
Akli	Lacustrine carbonaceous shale interlayered with coal, siltstones, and finer sandstones
Thumbli	Lignite beds and carbonaceous shales
Paleocene–Eocene:	
Dharvi Dungar	Bentonitic clays, carbonaceous shales, and fine-grained sandstones deposited in lacustrine to marine environment
Paleocene:	
Barmer Hill	Shallow marine sandstones and conglomerates with carbonaceous shale in the basal part consisting of plant fossils interbedded with siltstones and siliceous mudstones; the upper part consists of porcellanite and volcanic ash beds (Bariyada Member)
Fatehgarh ^a	Basal unit consists of conglomerates and volcanic debris associated with local intrusives (Dandlawas Fm.); this is overlain by near-shoreface to shallow marine sandstone and siltstone deposited by braided to meandering channels; some trace fossils have been seen at a few places in the upper part of the sandstone unit
Cretaceous:	
Upper Cretaceous:	
Rageshwari/pre-Deccan/precursor-of-Deccan volcanics	Basaltic lava flow, pyroclastic deposition (Agni Member)
Lower Cretaceous:	
Ghaggar-Hakra	Deposited in a maturing-up fluvial system consisting of three sandstone units—Darjaniyon-Ki-Dhani (lower; mixed/poorly sorted, clast-supported pebbly conglomerate overlain by coarse-grained quartz arenite and cross-bedded channel fill deposits), Sarnoo (middle; consisting of reddish, well-sorted, clast-supported channel fill deposits), and Nosar (upper; yellow cross-bedded medium to very coarse grained)—separated by floodplain deposits consisting of siltstone beds
Karentia volcanics (early Aptian)	Basaltic flow, exposed in Sarnoo hill area
Jurassic:	
Upper and Middle Jurassic	Hiatus
Lower Jurassic:	
Lathi	Fluvial coarse-grained sandstones, conglomerates, and siltstones
Pre-Cambrian:	
Late Proterozoic ^b :	
Basement	Malani Series/Malani suite/Malani igneous province/Malani System/Malani Igneous Suite/Malani Group/Malani Rhyolite (Malani intrusion consists of three phases: extrusive phase of bimodal volcanism: mafic followed by felsic flows; intrusive phase of felsic granite plutons; and hypabyssal phase of basic and felsic dike intrusions along rift fractures) unconformably overlies the Archean-Proterozoic metasediments and granite gneisses

Sources. Pascoe (1960); Crawford and Compston (1969); Dasgupta (1975); Pandey and Dave (1998); Pandit et al. (1999); Sisodia and Singh (2000); Torsvik et al. (2001); Sisodia (2006); Sharma (2007); Compton (2009); Valdiya (2010); Guha et al. (2013); Beaumont et al. (2015); Dolson et al. (2015); Abdelaziz et al. (2016); Parihar et al. (2016).

^a The oldest units in this formation are from the upper Cretaceous.

^b 751–771 Ma (Torsvik et al. 2001); 745 ± 10 Ma (Crawford and Compston 1969).

REFERENCES CITED ONLY IN THE APPENDIX

- Chaliha, M.; Bose, M.; and Mukherjee, S. 2016. Grain size variation and its impact on dynamic behaviour of a field: a field wide study using well cuttings. Accessed December 12, 2016. http://hrms.phistream.com/Uploads/1243id_Grain%20Size%20Variation%20and%20its%20Impact%20on%20Dynamic%20Behaviour%20of%20a%20Field%20A%20field%20wide%20study%20using%20well%20cuttings.pdf.
- Crawford, A. R., and Compston, W. 1969. The age of the Vindhyan system of peninsular India. *Q. J. Geol. Soc. Lond.* 125:351–371.
- Dash, S.; Roy, S.; Konar, S.; Bandyopadhyay, A.; Kuila, U.; Bora, A. K.; Mishra, P.; and Mohapatra, P. 2016. Paleo-stress and in-situ stress states in Raageshwari Volcanic Formation, Central Basin High, Barmer Basin. Accessed December 12, 2016. http://hrms.phistream.com/Uploads/1053id_Paleo-stress%20and%20In-situ%20Stress%20States%20in%20Raageshwari%20Volcanic%20Formation%20Central%20Basin%20High%20Barmer%20Basin.pdf.
- Guha, R.; Chowdhury, M.; Singh, S.; and Herold, B. 2013. Application of geomechanics and rock property analysis for a tight oil reservoir development: a case study from Barmer Basin, India. Biennial International Conference and Exposition on Petroleum Geophysics, 10th. Kochi, Society of Petroleum Geophysicists. https://www.spgindia.org/10_biennial_form/P268.pdf.
- Pal, A.; Nazhri, A.; Phinney, E.; Sunder, V.; Goodlad, S.; and Dwivedi, N. 2016. Structural modelling of complex fault relationships: a volume based modelling approach. International Petroleum Technology Conference, 10th (Bangkok, 2016). Accessed December 12, 2016. <https://www.onepetro.org/conference-paper/IPTC-18663-MS>.
- Pandey, J., and Dave, A. 1998. Stratigraphy of Indian petroliferous basins. XVI Indian Colloquium on Micropalaeontology and Stratigraphy (Dehradun), Proc. Dona Paula, India, National Institute of Oceanography, 248 p.
- Parihar, V. S.; Nama, S. L.; Khichi, C. P.; Shekhawat, N. S.; Snehlata, M.; and Mathur, S. C. 2016. Near shore–shallow marine (Ophiomorpha and Margaritichnus) trace fossils from Fatehgarh Formation of Barmer Basin, western Rajasthan, India. *J. Ecosyst. Ecogr.* 6:180. doi:10.4172/2157-7625.1000180.
- Pascoe, E. H. 1960. Manual of the geology of India and Burma. Calcutta, Geol. Surv. India, p. 553–560.
- Passchier, C. W., and Trouw, R. A. J. 2005. *Microtectonics* (2nd ed.). Berlin, Springer.
- Sisodia, M. S. 2006. Stratigraphy of Barmer Basin, Rajasthan: implication on Cretaceous-Tertiary boundary. *J. Geol. Soc. India* 67:828–829.
- Tiwari, A.; Harshvardhan; Mukherjee, S.; Keidel, S.; Goodlad, S.; Kumar, S.; and Ghosh, A. 2014. Updating the reservoir structural model through integrated interpretation of seismic, well, and dynamic data: a case study from the Bhagyam Field, Rajasthan, India. Society of Exploration Geophysicists International Exposition and Annual Meeting, 84th (Denver, CO, 2014), Tech. Program Expand. Abstr., p. 1533–1537. Tulsa, OK, Society of Exploration Geophysicists. doi:10.1190/segam2014-1334.1.

q54

q55